Hindawi Publishing Corporation
International Journal of Antennas and Propagation
Volume 2016, Article ID 9170403, 11 pages
http://dx.doi.org/10.1155/2016/9170403

Research Article

Separate DOD and DOA Estimation for Bistatic MIMO Radar

Lin Li,[1] Fangfang Chen,[1] and Jisheng Dai[1,2]

[1]*School of Electrical and Information Engineering, Jiangsu University, 301 Xuefu Road, Zhenjiang 212013, China*
[2]*National Mobile Communications Research Laboratory, Southeast University, 2 Sipailou Road, Nanjing 210096, China*

Correspondence should be addressed to Jisheng Dai; jsdai@ujs.edu.cn

Received 26 February 2016; Revised 6 June 2016; Accepted 20 June 2016

Academic Editor: Qinghua Guo

A novel MUSIC-type algorithm is derived in this paper for the direction of departure (DOD) and direction of arrival (DOA) estimation in a bistatic MIMO radar. Through rearranging the received signal matrix, we illustrate that the DOD and the DOA can be separately estimated. Compared with conventional MUSIC-type algorithms, the proposed separate MUSIC algorithm can avoid the interference between DOD and DOA estimations effectively. Therefore, it is expected to give a better angle estimation performance and have a much lower computational complexity. Meanwhile, we demonstrate that our method is also effective for coherent targets in MIMO radar. Simulation results verify the efficiency of the proposed method, particularly when the signal-to-noise ratio (SNR) is low and/or the number of snapshots is small.

1. Introduction

Multiple-input multiple-output (MIMO) radar, which utilizes multiple antennas to simultaneously transmit diverse waveforms and receive reflected signals, has many potential advantages over the conventional phased-array radar [1–4]. Direction of departure (DOD) and direction of arrival (DOA) estimation [5–8] is a key issue in MIMO radar signal processing, and it has attracted a lot of attention. Many algorithms for DOD and DOA estimation have been established in the literatures [9–11]. By exploiting the invariance property of both the transmit array and the receive array, [12] developed a subspace method based on the classical rotational invariance techniques (ESPRIT) algorithm, but additional pair matching is required. To avoid pair matching, an improved ESPRIT algorithm was presented in [13], whose complexity is lower than the algorithm in [12]. A real-valued ESPRIT algorithm was proposed in [14], where all the complex computations are transformed into real-valued ones. As a consequence, it can further reduce the computational complexity and ameliorate the performance for DOD and DOA estimation. Moreover, a propagator method (PM) algorithm for DOD and DOA estimation for MIMO radar was investigated in [15], which can construct the signal subspace without the eigenvalue decomposition of covariance matrix. So, the PM algorithm has lower complexity than ESPRIT-type methods [12–14, 16, 17], but it has a low performance of DOD and DOA estimation.

It is well known that multiple signal classification (MUSIC) algorithms have better performance than ESPRIT-type and PM-type algorithms. It has been proved that two-dimension MUSIC (2D-MUSIC) algorithm can be used for DOD and DOA estimation in MIMO radar and has a good angle estimation accuracy; however, it requires high computation complexity. The method in [18] combines ESPRIT and root-MUSIC to achieve the compromise between the complexity and estimation performance. In [19], a reduced-dimension MUSIC (RD-MUSIC) algorithm was proposed for DOD and DOA estimation, which can reduce the computational cost by replacing the two-dimensional searching with one-dimensional searching. All these MUSIC-type algorithms [19–22] can pair DOD and DOA estimation automatically. However, none of them can avoid the interference between DOD and DOA estimations. For example, if DOA is first estimated in these methods, then the estimation of DOD will be influenced by the estimation error of DOA.

Therefore, the performance of these MUSIC-type algorithms might seriously degrade.

To solve the aforementioned problem, in this paper, a separate MUSIC algorithm for DOD and DOA estimation is presented. The algorithm first addresses the DOD estimation and then rearranges the received signal matrix to estimate DOA. Compared with conventional MUSIC-type algorithms, the proposed algorithm, due to the utilization of separate DOD and DOA estimation, avoids the interference between DOD and DOA estimations effectively; therefore, the algorithm gives a better angle estimation accuracy and has a much lower computational complexity, when signal-to-noise ratio (SNR) is low and/or the number of snapshots is small. Meanwhile, this paper guarantees that the algorithm is also effective for coherent targets in MIMO radar.

This paper is organized as follows. Section 2 addresses the data model for bistatic MIMO radar. Section 3 reviews the existing MUSIC-type algorithms for DOD and DOA estimation. Section 4 proposes our separate MUSIC algorithm for DOD and DOA estimation. Finally, simulation results and conclusions are given in Sections 5 and 6, respectively.

2. Data Model

Consider a bistatic MIMO radar system with M transmit antennas and N receive antennas, both of which are half-wavelength spaced uniform linear arrays (ULAs). At the transmit site, M different narrowband waveforms are emitted simultaneously, which have identical bandwidth and central frequency but are temporally orthogonal. In each receiver, the echoes are processed for all of the transmitted waveforms. Assume that there are P uncorrelated targets located at the same range, and the DOD and DOA of the pth target relative to the transmitter and the receiver are denoted by θ_p and φ_p, respectively.

The output of the matched filters at the receiver can be expressed as

$$\mathbf{x}(t) = \mathbf{A}\mathbf{s}(t) + \mathbf{n}(t), \tag{1}$$

where $\mathbf{A} = [\mathbf{a}_r(\varphi_1) \otimes \mathbf{a}_t(\theta_1), \ldots, \mathbf{a}_r(\varphi_P) \otimes \mathbf{a}_t(\theta_P)]$ is an $NM \times P$ array manifold matrix with

$$\begin{aligned} &\mathbf{a}_r(\varphi_p) \\ &\quad = \left[1, \exp\left(j\pi \sin\varphi_p\right), \ldots, \exp\left(j\pi (M-1) \sin\varphi_p\right)\right]^T, \\ &\qquad\qquad p = 1, 2, \ldots, P, \\ &\mathbf{a}_t(\theta_p) \\ &\quad = \left[1, \exp\left(j\pi \sin\theta_p\right), \ldots, \exp\left(j\pi (N-1) \sin\theta_p\right)\right]^T, \\ &\qquad\qquad p = 1, 2, \ldots, P \end{aligned} \tag{2}$$

being the receive steering vector and the transmit steering vector, respectively. $\otimes$ is the Kronecker product and $[\cdot]^T$ is the transpose operation. $\mathbf{s}(t) = [s_1(t), s_2(t), \ldots, s_P(t)]^T$ is a column vector consisting of the amplitudes and phases of the P targets at time t. $\mathbf{n}(t)$ represents an $NM \times 1$ complex Gaussian white noise vector of zeros mean and covariance matrix $\sigma^2 \mathbf{I}_{NM}$.

3. Review of MUSIC-Type Algorithms

Let $\mathbf{X}$ be denoted as the data matrix composed of L snapshots of $\mathbf{x}(t_l)$, $1 \le l \le L$; then the $NM \times L$ matrix $\mathbf{X}$ can be expressed as

$$\mathbf{X} = \mathbf{A}\mathbf{S} + \mathbf{N}, \tag{3}$$

where

$$\begin{aligned} \mathbf{S} &= \begin{bmatrix} s_1(t_1) & s_1(t_2) & \cdots & s_1(t_L) \\ s_2(t_1) & s_2(t_2) & \cdots & s_2(t_L) \\ \vdots & \vdots & \ddots & \vdots \\ s_P(t_1) & s_P(t_2) & \cdots & s_P(t_L) \end{bmatrix}, \\ \mathbf{N} &= \begin{bmatrix} n_1(t_1) & n_1(t_2) & \cdots & n_1(t_L) \\ n_2(t_1) & n_2(t_2) & \cdots & n_2(t_L) \\ \vdots & \vdots & \ddots & \vdots \\ n_{NM}(t_1) & n_{NM}(t_2) & \cdots & n_{NM}(t_L) \end{bmatrix}. \end{aligned} \tag{4}$$

The covariance matrix of $\mathbf{X}$ is defined as

$$\mathbf{R} = \frac{1}{L}\mathbf{X}\mathbf{X}^H = \mathbf{A}\mathbf{R}_s\mathbf{A}^H + \sigma^2\mathbf{I}_{NM}, \tag{5}$$

where $\mathbf{R}_S = (1/L)\mathbf{S}\mathbf{S}^H$ is the source covariance matrix and $[\cdot]^H$ is the Hermitian transpose. Let the eigenvalue decomposition of $\mathbf{R}$ be

$$\mathbf{R} = \mathbf{U}_s\mathbf{\Sigma}_s\mathbf{U}_s^H + \mathbf{U}_n\mathbf{\Sigma}_n\mathbf{U}_n^H, \tag{6}$$

where $\mathbf{\Sigma}_s$ denotes a $P \times P$ diagonal matrix formed by P largest eigenvalues and $\mathbf{\Sigma}_n$ denotes a diagonal matrix formed by the rest of the $NM - P$ smaller eigenvalues. $\mathbf{U}_s$ and $\mathbf{U}_n$ represent the signal subspace and noise subspace, respectively, of which $\mathbf{U}_s$ contains the eigenvectors corresponding to the P largest eigenvalues and $\mathbf{U}_n$ consists of the rest of the eigenvectors. As the noise subspace $\mathbf{U}_n$ is orthogonal to the actual target directional vector, we can construct the 2D-MUSIC spatial spectrum function as follows:

$$\begin{aligned} &P_{\text{2D-MUSIC}}(\varphi, \theta) \\ &\quad = \frac{1}{[\boldsymbol{\alpha}_r(\varphi) \otimes \boldsymbol{\alpha}_t(\theta)]^H \mathbf{U}_n\mathbf{U}_n^H [\boldsymbol{\alpha}_r(\varphi) \otimes \boldsymbol{\alpha}_t(\theta)]}. \end{aligned} \tag{7}$$

Here, we have the P largest peaks of $P_{\text{2D-MUSIC}}(\varphi, \theta)$ corresponding to the estimates of the DODs and DOAs for the targets.

Since 2D-MUSIC requires exhaustive two-dimensional searching, it is normally inefficient due to high computational cost, and therefore Zhang et al. [19] proposed a RD-MUSIC

algorithm which has a much lower computational complexity. Firstly, let

$$\mathbf{V}(\varphi,\theta) = [\boldsymbol{\alpha}_r(\varphi)\otimes\boldsymbol{\alpha}_t(\theta)]^H \mathbf{U}_n\mathbf{U}_n^H [\boldsymbol{\alpha}_r(\varphi)\otimes\boldsymbol{\alpha}_t(\theta)]. \quad (8)$$

Then, the RD-MUSIC algorithm rewrites $\mathbf{V}(\varphi,\theta)$ as

$$\begin{aligned}\mathbf{V}(\varphi,\theta) &= \boldsymbol{\alpha}_t(\theta)^H [\boldsymbol{\alpha}_r(\varphi)\otimes\mathbf{I}_M]^H \mathbf{U}_n\mathbf{U}_n^H [\boldsymbol{\alpha}_r(\varphi)\otimes\mathbf{I}_M]\boldsymbol{\alpha}_t(\theta) \quad (9)\\ &= \boldsymbol{\alpha}_t(\theta)^H \mathbf{Q}(\varphi)\boldsymbol{\alpha}_t(\theta).\end{aligned}$$

The DOAs can be found from the quadratic optimization problem $\min_{\varphi,\theta}\boldsymbol{\alpha}_t(\theta)^H\mathbf{Q}(\varphi)\boldsymbol{\alpha}_t(\theta)$. In order to avoid a trivial zero solution, some normalized constraint (e.g., $\mathbf{e}_1^H\mathbf{a}_t(\theta)=1$, where $\mathbf{e}_1 = [1,0,\ldots,0]^T \in R^{M\times 1}$) should be added to the optimization problem; that is,

$$\begin{aligned}\min_{\varphi,\theta}\quad & \boldsymbol{\alpha}_t(\theta)^H \mathbf{Q}(\varphi)\boldsymbol{\alpha}_t(\theta),\\ \text{s.t.}\quad & \mathbf{e}_1^H\mathbf{a}_t(\theta)=1.\end{aligned} \quad (10)$$

According to the Karush-Kuhn-Tucker (KKT) conditions, we have

$$\mathbf{a}_t(\theta) = \frac{\mathbf{Q}(\varphi)^{-1}\mathbf{e}_1}{\mathbf{e}_1^H\mathbf{Q}(\varphi)^{-1}\mathbf{e}_1}. \quad (11)$$

Inserting (11) into the objective function $\boldsymbol{\alpha}_t(\theta)^H\mathbf{Q}(\varphi)\boldsymbol{\alpha}_t(\theta)$, DOAs can be estimated via

$$\widetilde{\varphi} = \arg\min_{\varphi}\frac{1}{\mathbf{e}_1^H\mathbf{Q}(\varphi)^{-1}\mathbf{e}_1} = \arg\max_{\varphi}\mathbf{e}_1^H\mathbf{Q}(\varphi)^{-1}\mathbf{e}_1. \quad (12)$$

Searching the objective function of $\mathbf{e}_1^H\mathbf{Q}(\varphi)^{-1}\mathbf{e}_1$ along $\varphi \in [-90^\circ, 90^\circ]$, we can find the P largest peaks that correspond to DOAs $(\widetilde{\varphi}_1,\widetilde{\varphi}_2,\ldots,\widetilde{\varphi}_P)$. Substituting (11) for the estimated DOAs $\widetilde{\varphi}_1,\widetilde{\varphi}_2,\ldots,\widetilde{\varphi}_P$, we may obtain P vectors $\widetilde{\mathbf{a}}_t(\theta_1),\widetilde{\mathbf{a}}_t(\theta_2),\ldots,\widetilde{\mathbf{a}}_t(\theta_P)$. Finally, the DODs can be found after some algebraic calculation with $\widetilde{\mathbf{a}}_t(\theta_1),\widetilde{\mathbf{a}}_t(\theta_2),\ldots,\widetilde{\mathbf{a}}_t(\theta_P)$.

4. Separate MUSIC Algorithm for DOD and DOA Estimation

Obviously, the DOD estimation of RD-MUSIC algorithm is based on the estimate of the DOA. It is likely to degrade the DOD estimation performance due to the interference caused by the DOA estimation. In this section, we will propose a separate MUSIC algorithm to handle the problem. To this end, we first address the DOD estimation and then rearrange the received signal matrix $\mathbf{X}$ to estimate DOA. Finally, we will address the pair matching.

4.1. DOD Estimation. In order to simplify the notation, we rewrite $\mathbf{a}_r(\varphi_p) = [1, z_{rp}, z_{rp}^2,\ldots,z_{rp}^{N-1}]^T$ with $z_{rp} = \exp(j\pi\sin\varphi_p)$. Then, the array manifold matrix $\mathbf{A}$ becomes

$$\mathbf{A} = \begin{bmatrix} \mathbf{a}_t(\theta_1) & \mathbf{a}_t(\theta_2) & \cdots & \mathbf{a}_t(\theta_P)\\ z_{r1}\mathbf{a}_t(\theta_1) & z_{r2}\mathbf{a}_t(\theta_2) & \cdots & z_{rP}\mathbf{a}_t(\theta_P)\\ \vdots & \vdots & \ddots & \vdots\\ z_{r1}^{N-1}\mathbf{a}_t(\theta_1) & z_{r2}^{N-1}\mathbf{a}_t(\theta_2) & \cdots & z_{rP}^{N-1}\mathbf{a}_t(\theta_P)\end{bmatrix}. \quad (13)$$

We partition the matrix $\mathbf{X}$, defined in (3), into N submatrices:

$$\mathbf{X} = \begin{bmatrix}\mathbf{X}_1\\ \mathbf{X}_2\\ \vdots\\ \mathbf{X}_N\end{bmatrix} = \begin{bmatrix}\mathbf{A}_1\mathbf{S}\\ \mathbf{A}_2\mathbf{S}\\ \vdots\\ \mathbf{A}_N\mathbf{S}\end{bmatrix} + \begin{bmatrix}\mathbf{N}_1\\ \mathbf{N}_2\\ \vdots\\ \mathbf{N}_N\end{bmatrix}, \quad (14)$$

where

$$\begin{aligned}\mathbf{X}_n &= \mathbf{A}_n\mathbf{S} + \mathbf{N}_n,\\ \mathbf{A}_n &= [z_{r1}^{n-1}\mathbf{a}_t(\theta_1)\ \ z_{r2}^{n-1}\mathbf{a}_t(\theta_2)\ \ \cdots\ \ z_{rP}^{n-1}\mathbf{a}_t(\theta_P)]\\ &= \underbrace{[\mathbf{a}_t(\theta_1)\ \ \mathbf{a}_t(\theta_2)\ \ \cdots\ \ \mathbf{a}_t(\theta_P)]}_{\triangleq\mathbf{A}_t}\operatorname{diag}\underbrace{[z_{r1}^{n-1}, z_{r2}^{n-1},\ldots,z_{rP}^{n-1}]}_{\triangleq\boldsymbol{\Phi}_r^{n-1}}\\ &= \mathbf{A}_t\boldsymbol{\Phi}_r^{n-1},\\ \mathbf{N}_n &= \begin{bmatrix} n_{(n-1)M+1}(t_1) & n_{(n-1)M+1}(t_2) & \cdots & n_{(n-1)M+1}(t_L)\\ n_{(n-1)M+2}(t_1) & n_{(n-1)M+2}(t_2) & \cdots & n_{(n-1)M+2}(t_L)\\ \vdots & \vdots & \ddots & \vdots\\ n_{nM}(t_1) & n_{nM}(t_2) & \cdots & n_{nM}(t_L)\end{bmatrix},\end{aligned} \quad (15)$$

and diag[$\mathbf{v}$] denotes a diagonal matrix constructed by the vector $\mathbf{v}$.

In order to independently estimate DOD, we construct a new matrix containing the information of DOD; that is,

$$\mathbf{X}_t = [\mathbf{X}_1, \mathbf{X}_2,\ldots,\mathbf{X}_N]. \quad (16)$$

According to the structure of $\mathbf{X}$ in (14), $\mathbf{X}_t$ can be rewritten by

$$\begin{aligned}\mathbf{X}_t &= [\mathbf{A}_t\mathbf{S}, \mathbf{A}_t\boldsymbol{\Phi}_r\mathbf{S},\ldots,\mathbf{A}_t\boldsymbol{\Phi}_r^{N-1}\mathbf{S}] + \underbrace{[\mathbf{N}_1,\mathbf{N}_2,\ldots,\mathbf{N}_N]}_{\triangleq\mathbf{N}_t}\\ &= \mathbf{A}_t\underbrace{[\mathbf{S}, \boldsymbol{\Phi}_r\mathbf{S},\ldots,\boldsymbol{\Phi}_r^{N-1}\mathbf{S}]}_{\triangleq\mathbf{S}_t} + \mathbf{N}_t = \mathbf{A}_t\mathbf{S}_t + \mathbf{N}_t.\end{aligned} \quad (17)$$

Note that $\mathbf{S}_t$ and $\mathbf{N}_t$ can be seen as the signal matrix and noise matrix corresponding to the new measurement matrix $\mathbf{X}_t$, respectively.

The covariance matrix of $\mathbf{X}_t$ is defined as

$$\begin{aligned}\mathbf{R}_t &= \frac{1}{L}\mathbf{X}_t\mathbf{X}_t^H \\ &= \frac{1}{L}\mathbf{A}_t\left[\mathbf{S}, \mathbf{\Phi}_r\mathbf{S}, \ldots, \mathbf{\Phi}_r^{N-1}\mathbf{S}\right]\begin{bmatrix}\mathbf{S}^H \\ \mathbf{S}^H\mathbf{\Phi}_r^H \\ \vdots \\ \mathbf{S}^H\left(\mathbf{\Phi}_r^{N-1}\right)^H\end{bmatrix}\mathbf{A}_t^H \\ &\quad + \sigma^2\mathbf{I}_M,\end{aligned} \tag{18}$$

where $\mathbf{R}_{ts} = (1/L)\sum_{n=1}^{N}\mathbf{\Phi}_r^{n-1}\mathbf{S}\mathbf{S}^H(\mathbf{\Phi}_r^{n-1})^H$ is the source covariance matrix corresponding to $\mathbf{X}_t$. Performing the eigenvalue decomposition of $\mathbf{R}_t$, we can get the noise subspace $\mathbf{U}_{nt}$ corresponding to $\mathbf{X}_t$. Then, we construct the following MUSIC spatial spectrum function for DOD estimation:

$$P_t(\theta) = \frac{1}{\mathbf{a}_t^H(\theta)\,\mathbf{U}_{nt}\mathbf{U}_{nt}^H\mathbf{a}_t(\theta)}. \tag{19}$$

Searching $\theta \in [-90^\circ, 90^\circ]$, we can obtain P largest peaks of $P_t(\theta)$. The corresponding $(\widehat{\theta}_1, \widehat{\theta}_2, \ldots, \widehat{\theta}_P)$ are taken as the estimates of the DODs.

Actually, our method is effective for coherent DOD estimation. Considering a completely coherent environment [23–25], we have

$$s_p(t) = \alpha_p s_1(t), \quad p = 1, 2, \ldots, P, \tag{20}$$

where α_p ($\alpha_p \neq 0$) represents the complex attenuation of the pth signal with respect to the first signal $s_1(t)$. Using (20) with $E[s_1^2(t_l)] = 1$, $l = 1, 2, \ldots, L$, it is easy to see that

$$\mathbf{R}_s = \boldsymbol{\alpha}\boldsymbol{\alpha}^H, \tag{21}$$

where $\boldsymbol{\alpha} = [\alpha_1, \alpha_1, \ldots, \alpha_P]^T$. So the source covariance matrix $\mathbf{R}_{ts}$ takes the form [26]

$$\begin{aligned}\mathbf{R}_{ts} &= \frac{1}{L}\sum_{n=1}^{N}\mathbf{\Phi}_r^{n-1}\mathbf{S}\mathbf{S}^H\left(\mathbf{\Phi}_r^{n-1}\right)^H \\ &= \frac{1}{L}\sum_{n=1}^{N}\mathbf{\Phi}_r^{n-1}\boldsymbol{\alpha}\boldsymbol{\alpha}^H\left(\mathbf{\Phi}_r^{n-1}\right)^H = \frac{1}{L}\mathbf{B}\mathbf{B}^H,\end{aligned} \tag{22}$$

where

$$\begin{aligned}\mathbf{B} &= \left[\boldsymbol{\alpha}, \mathbf{\Phi}_r\boldsymbol{\alpha}, \ldots, \mathbf{\Phi}_r^{N-1}\boldsymbol{\alpha}\right] \\ &= \begin{bmatrix}\alpha_1 & & & \\ & \alpha_2 & & \\ & & \ddots & \\ & & & \alpha_P\end{bmatrix}\begin{bmatrix}1 & z_{r1} & \cdots & z_{r1}^{N-1} \\ 1 & z_{r2} & \cdots & z_{r2}^{N-1} \\ \vdots & \vdots & \ddots & \vdots \\ 1 & z_{rP} & \cdots & z_{rP}^{N-1}\end{bmatrix} \triangleq \mathbf{D}\mathbf{V}.\end{aligned} \tag{23}$$

Clearly, the rank of $\mathbf{R}_{ts}$ is equal to the rank of $\mathbf{B}$. Since $\mathbf{B} = \mathbf{D}\mathbf{V}$ and the diagonal matrix $\mathbf{D}$ is of full rank, the rank of $\mathbf{B}$ is the same as that of $\mathbf{V}$. Now, the rank of the $P \times N$ Vandermonde matrix $\mathbf{V}$ is $\operatorname{rank}(\mathbf{V}) = \min(P, N)$, and, hence, $\operatorname{rank}(\mathbf{V}) = P$ if $N \geq P$. We can find that the rank of $\mathbf{R}_t$ is the same as the number of the targets. Therefore, the proposed algorithm can be applied to solve multiple coherent targets for DOD estimation.

4.2. DOA Estimation. Define a new $MN \times P$ matrix $\mathbf{A}' = [\mathbf{a}_1', \mathbf{a}_2', \ldots, \mathbf{a}_P']$, where $\mathbf{a}_p' = \mathbf{a}_t(\theta_p) \otimes \mathbf{a}_r(\varphi_p)$. In order to simplify the notation, we rewrite $\mathbf{a}_t(\theta) = [1, z_{tp}, z_{tp}^2, \ldots, z_{tp}^{M-1}]$ with $z_{tp} = \exp(j\pi\sin\theta_p)$; then, we have

$$\begin{aligned}&\mathbf{A}' \\ &= \begin{bmatrix}\mathbf{a}_r(\varphi_1) & \mathbf{a}_r(\varphi_2) & \cdots & \mathbf{a}_r(\varphi_P) \\ z_{t1}\mathbf{a}_r(\varphi_1) & z_{t2}\mathbf{a}_r(\varphi_2) & \cdots & z_{tP}\mathbf{a}_r(\varphi_P) \\ \vdots & \vdots & \ddots & \vdots \\ z_{t1}^{M-1}\mathbf{a}_r(\varphi_1) & z_{t2}^{M-1}\mathbf{a}_r(\varphi_2) & \cdots & z_{tP}^{M-1}\mathbf{a}_r(\varphi_P)\end{bmatrix}.\end{aligned} \tag{24}$$

Obviously, there exists an $NM \times NM$ transformation matrix $\mathbf{B}$ corresponding to the finite number of row interchanged operations such that $\mathbf{A}' = \mathbf{B}\mathbf{A}$, where

$$\begin{aligned}\mathbf{B} &= \begin{bmatrix}b_{11} & b_{12} & \cdots & b_{1,MN} \\ b_{21} & b_{22} & \cdots & b_{2,MN} \\ \vdots & \vdots & \vdots & \vdots \\ b_{MN,1} & b_{MN,2} & \cdots & b_{MN,MN}\end{bmatrix}_{MN\times MN}, \\ b_{ij} &= \begin{cases}1, & i = g + (h-1)N,\ j = h + (g-1)M \\ 0, & \text{others},\end{cases} \quad g = 1, 2, \ldots, N,\ h = 1, 2, \ldots, M.\end{aligned} \tag{25}$$

Using the structure of the matrix $\mathbf{A}'$, we introduce a virtual $MN \times P$ data matrix $\mathbf{X}' \triangleq \mathbf{BX}$, or, equivalently,

$$\mathbf{X}' = \mathbf{A}'\mathbf{S} + \mathbf{N}', \tag{26}$$

where $\mathbf{N}' \triangleq \mathbf{BN}$. Divide the matrix $\mathbf{X}'$ into M submatrices:

$$\mathbf{X}' = \begin{bmatrix} \mathbf{X}'_1 \\ \mathbf{X}'_2 \\ \vdots \\ \mathbf{X}'_M \end{bmatrix} = \begin{bmatrix} \mathbf{A}'_1\mathbf{S} \\ \mathbf{A}'_2\mathbf{S} \\ \vdots \\ \mathbf{A}'_M\mathbf{S} \end{bmatrix} + \begin{bmatrix} \mathbf{N}'_1 \\ \mathbf{N}'_2 \\ \vdots \\ \mathbf{N}'_M \end{bmatrix}, \tag{27}$$

where

$$\begin{aligned}
\mathbf{X}'_m &= \mathbf{A}'_m\mathbf{S} + \mathbf{N}'_m, \\
\mathbf{A}'_m &= \left[z_{t1}^{m-1}\mathbf{a}_r(\varphi_1) \;\; z_{t2}^{m-1}\mathbf{a}_r(\varphi_2) \;\; \cdots \;\; z_{tP}^{m-1}\mathbf{a}_r(\varphi_P)\right] \\
&= \underbrace{\left[\mathbf{a}_r(\varphi_1) \;\; \mathbf{a}_r(\varphi_2) \;\; \cdots \;\; \mathbf{a}_r(\varphi_P)\right]}_{\triangleq \mathbf{A}_r}\operatorname{diag}\underbrace{\left[z_{t1}^{m-1} \;\; z_{t2}^{m-1} \;\; \cdots \;\; z_{tP}^{m-1}\right]}_{\triangleq \mathbf{\Phi}_t^{m-1}} \\
&= \mathbf{A}_r\mathbf{\Phi}_t^{m-1},
\end{aligned} \tag{28}$$

$$\mathbf{N}'_m = \begin{bmatrix} n'_{(m-1)N+1}(t_1) & n'_{(m-1)N+1}(t_2) & \cdots & n'_{(m-1)N+1}(t_L) \\ n'_{(m-1)N+2}(t_1) & n'_{(m-1)N+2}(t_2) & \cdots & n'_{(m-1)N+2}(t_L) \\ \vdots & \vdots & \ddots & \vdots \\ n'_{mN}(t_1) & n'_{mN}(t_2) & \cdots & n'_{mN}(t_L) \end{bmatrix}.$$

In order to estimate DOA independently, we construct a new $N \times ML$ matrix $\mathbf{X}_r$:

$$\mathbf{X}_r = \left[\mathbf{X}'_1, \mathbf{X}'_2, \ldots, \mathbf{X}'_M\right] \tag{29}$$

which contains the information of DOA. According to the structure of $\mathbf{X}'$ in (27), $\mathbf{X}_r$ can be expressed as

$$\begin{aligned}
\mathbf{X}_r &= \left[\mathbf{A}_r\mathbf{S}, \mathbf{A}_r\mathbf{\Phi}_t\mathbf{S}, \ldots, \mathbf{A}_r\mathbf{\Phi}_t^{M-1}\mathbf{S}\right] \\
&\quad + \underbrace{\left[\mathbf{N}'_1, \mathbf{N}'_2, \ldots, \mathbf{N}'_M\right]}_{\triangleq \mathbf{N}_r} \\
&= \mathbf{A}_r\underbrace{\left[\mathbf{I}_P\mathbf{S}, \mathbf{\Phi}_t\mathbf{S}, \ldots, \mathbf{\Phi}_t^{M-1}\mathbf{S}\right]}_{\triangleq \mathbf{S}_r} + \mathbf{N}_r = \mathbf{A}_r\mathbf{S}_r + \mathbf{N}_r.
\end{aligned} \tag{30}$$

Note that $\mathbf{S}_r$ and $\mathbf{N}_r$ can be seen as the virtual signal matrix and noise matrix corresponding to the measurement $\mathbf{X}_r$, respectively. The covariance matrix of $\mathbf{X}_r$ can be calculated by

$$\begin{aligned}
\mathbf{R}_r &= \frac{1}{L}\mathbf{X}_r\mathbf{X}_r^H \\
&= \frac{1}{L}\mathbf{A}_r\left[\mathbf{S}_r, \mathbf{\Phi}_t\mathbf{S}_r, \ldots, \mathbf{\Phi}_t^{M-1}\mathbf{S}_r\right]\begin{bmatrix} \mathbf{S}_r^H \\ \mathbf{S}_r^H\mathbf{\Phi}_t^H \\ \vdots \\ \mathbf{S}_r^H\left(\mathbf{\Phi}_t^{M-1}\right)^H \end{bmatrix}\mathbf{A}_r^H \\
&\quad + \sigma^2\mathbf{I}_N \\
&= \frac{1}{L}\mathbf{A}_r\left(\sum_{m=1}^{M}\mathbf{\Phi}_t^{m-1}\mathbf{S}_r\mathbf{S}_r^H\left(\mathbf{\Phi}_t^{m-1}\right)^H\right)\mathbf{A}_r^H + \sigma^2\mathbf{I}_N \\
&= \mathbf{A}_r\mathbf{R}_{rs}\mathbf{A}_r^H + \sigma^2\mathbf{I}_N,
\end{aligned} \tag{31}$$

where $\mathbf{R}_{rs} = (1/L)\sum_{m=1}^{M}\mathbf{\Phi}_t^{m-1}\mathbf{S}_r\mathbf{S}_r^H(\mathbf{\Phi}_t^{m-1})^H$ is the source covariance matrix corresponding to $\mathbf{X}_r$. Performing the eigenvalue decomposition of $\mathbf{R}_r$, we obtain the noise subspace matrix $\mathbf{U}_{nr}$ of $\mathbf{X}_r$. Thus, the MUSIC spatial spectrum function for DOA estimation can be expressed as

$$P_r(\varphi) = \frac{1}{\mathbf{a}_r^H(\varphi)\mathbf{U}_{nr}\mathbf{U}_{nr}^H\mathbf{a}_r(\varphi)}. \tag{32}$$

Searching $\varphi \in [-90^\circ, 90^\circ]$, we obtain the P largest peaks of $P_r(\varphi)$ corresponding to the estimated DOAs $(\widehat{\varphi}_1, \widehat{\varphi}_2, \ldots, \widehat{\varphi}_P)$. Moreover, since $\mathbf{R}_r$ has similar structure characteristics to $\mathbf{R}_t$, the rank of $\mathbf{R}_r$ is also the same as the number of the targets. Therefore, the proposed algorithm can also be applied to solve multiple coherent targets for DOA estimation.

4.3. Pair Matching for DOD and DOA. Now, the estimates of DODs and DOAs have been acquired from the functions $P_t(\theta)$ and $P_r(\varphi)$. Then, we form easily P vectors $\mathbf{a}_t(\widehat{\theta}_1), \mathbf{a}_t(\widehat{\theta}_2), \ldots, \mathbf{a}_t(\widehat{\theta}_P)$ and P vectors $\mathbf{a}_r(\widehat{\varphi}_1)$, $\mathbf{a}_r(\widehat{\varphi}_2), \ldots, \mathbf{a}_r(\widehat{\varphi}_P)$, respectively. The paired DOD and DOA, denoted by $(\widehat{\theta}_p, \widehat{\varphi}_{\pi_p})$, where $p = 1, 2, \ldots, P$ and $\pi_p \in \{1, 2, \ldots, P\}$, maximize the spatial spectrum function (7):

$$\begin{aligned}
&P\left(\widehat{\theta}_i, \widehat{\varphi}_j\right) \\
&\quad = \frac{1}{\left[\mathbf{a}_r\left(\widehat{\varphi}_j\right) \otimes \mathbf{a}_t\left(\widehat{\theta}_i\right)\right]^H\mathbf{U}_n\mathbf{U}_n^H\left[\mathbf{a}_r\left(\widehat{\varphi}_j\right) \otimes \mathbf{a}_t\left(\widehat{\theta}_i\right)\right]}.
\end{aligned} \tag{33}$$

Summarily, we show the major steps of our proposed algorithm as follows.

Step 1. Form $\mathbf{X}_t$ and $\mathbf{X}_r$ according to (16) and (29).

Step 2. Calculate the sample covariance matrix of $\mathbf{X}_t$ and $\mathbf{X}_r$, respectively, and obtain the noise subspace matrices $\mathbf{U}_{nt}$ and $\mathbf{U}_{nr}$ correspondingly.

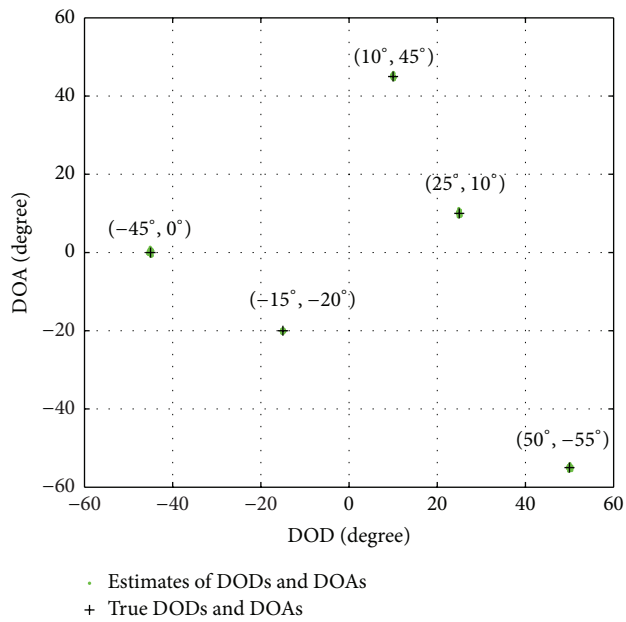

Figure 1: Paired results of the proposed algorithm for all five targets.

Step 3. Acquire the estimates of DODs and DOAs by searching θ through (19) and φ through (32), respectively.

Step 4. Pair the estimates of DODs and DOAs with (33).

5. Simulation Results

In this section, we introduce the simulation results of the proposed algorithm in comparison with the standard ESPRIT method [13], the Unitary ESPRIT method [14], the RD-MUSIC method [19], and the PM method [15]. The root mean squared error (RMSE) of the DOD or DOA estimation is defined as

$$\text{RMSE} = \frac{1}{P}\sum_{p=1}^{P}\sqrt{\frac{1}{200}\sum_{n=1}^{200}\left(\widehat{\beta}_{p,n}-\beta_p\right)^2}, \tag{34}$$

where $\widehat{\beta}_{p,n}$ is the estimate of DOD or DOA corresponding to true value β_p of DOD or DOA of the nth Monte Carlo trial. In the following simulations, we adopt the 200 Monte Carlo trials for a bistatic MIMO radar system with uniform linear arrays with half-wavelength spacing.

Simulation 1 presents the angle paired results of the proposed algorithm. In this simulation, we assume a ULA composed of $M = 10$ transmit antennas and $N = 8$ receive antennas, and we consider $P = 5$ uncorrelated targets located at angles $(\theta_1, \varphi_1) = (-45^\circ, 0^\circ)$, $(\theta_2, \varphi_2) = (-15^\circ, -20^\circ)$, $(\theta_3, \varphi_3) = (10^\circ, 45^\circ)$, $(\theta_4, \varphi_4) = (25^\circ, 10^\circ)$, and $(\theta_5, \varphi_5) = (50^\circ, -55^\circ)$, respectively. The number of snapshots is $L = 20$, and the SNR is 0 dB. As can be seen from Figure 1, the proposed algorithm can correctly estimate and pair the DODs and DOAs.

Simulation 2 shows the performance of RMSE versus SNR for the DOD and DOA estimation of the proposed algorithm in comparison with the standard ESPRIT method, the Unitary ESPRIT method, the RD-MUSIC method, and the PM method. In this simulation, the number of snapshots is $L = 10$. We assume a ULA composed of $M = 10$ transmit antennas and $N = 10$ receive antennas, and we consider $P = 4$ uncorrelated targets located at angles $(\theta_1, \varphi_1) = (-15^\circ, -15^\circ)$, $(\theta_2, \varphi_2) = (6^\circ, 10^\circ)$, $(\theta_3, \varphi_3) = (50^\circ, 50^\circ)$, and $(\theta_4, \varphi_4) = (-45^\circ, 25^\circ)$, respectively. Figure 2(a) depicts DOD estimation performance of RMSE versus SNR. Figure 2(b) presents DOA estimation performance of RMSE versus SNR. As shown in the figure, the proposed algorithm has much better DOD and DOA estimation performance than other algorithms, particularly at the low SNR. Furthermore, we use the Cramer-Rao bound (CRB), calculated in the Appendix, as the performance benchmark. Obviously, the performance of the proposed algorithm is closer to the CRB than others.

Simulation 3 is used to verify whether our method can improve the interference between DOD and DOA estimations, where we compare it with the RD-MUSIC method and the CRB. In this simulation, we use the same parameters as in Simulation 2. As shown in Figure 3, obviously, the DOA estimation has a little influence on the DOD estimation of the proposed algorithm; however, the RD-MUSIC algorithm has large interference between DOD and DOA estimations. Hence, we have a conclusion that the proposed algorithm, owing to utilizing the separate DOD and DOA estimation, reduces the interference between DOD and DOA estimations and thus improves the accuracy of DOD and DOA estimation. Furthermore, the performance of the proposed algorithm is closer to the CRB than the RD-MUSIC method.

Simulation 4 shows the DOD and DOA estimation performance of the proposed algorithm with different snapshots L. We consider a ULA composed of $M = 12$ transmit antennas and $N = 12$ receive antennas, and we assume $P = 3$ uncorrelated targets located at angles $(\theta_1, \varphi_1) = (-25^\circ, -20^\circ)$, $(\theta_2, \varphi_2) = (0^\circ, 45^\circ)$, and $(\theta_3, \varphi_3) = (45^\circ, 5^\circ)$, respectively. Figure 4(a) depicts DOD estimation performance of RMSE versus different number of snapshots L. Figure 4(b) presents DOA estimation performance of RMSE versus different number of snapshots L. As indicated in the figure, the performance of the proposed algorithm for DOD and DOA estimation is improved with L increasing, and we also draw a conclusion that the proposed algorithm works well in the case of small sampling sizes (e.g., $L = 10$).

Simulation 5 illustrates the achieved performance of the proposed algorithm with different transmit antennas and receive antennas for DOD and DOA estimation. In this simulation, the number of snapshots is $L = 50$. We consider $P = 3$ uncorrelated targets located at angles $(\theta_1, \varphi_1) = (-35^\circ, -20^\circ)$, $(\theta_2, \varphi_2) = (9^\circ, 45^\circ)$, and $(\theta_3, \varphi_3) = (55^\circ, 10^\circ)$, respectively. Figures 5(a) and 5(b) depict DOD and DOA estimation performance of RMSE versus different number of transmit antennas M under $N = 10$ condition, respectively. Figures 6(a) and 6(b) present DOD and DOA estimation performance of RMSE versus different number of transmit antennas N under $M = 10$ condition, respectively. It is clearly shown in Figures 5 and 6 that the angle estimation performance of the proposed algorithm is gradually improved

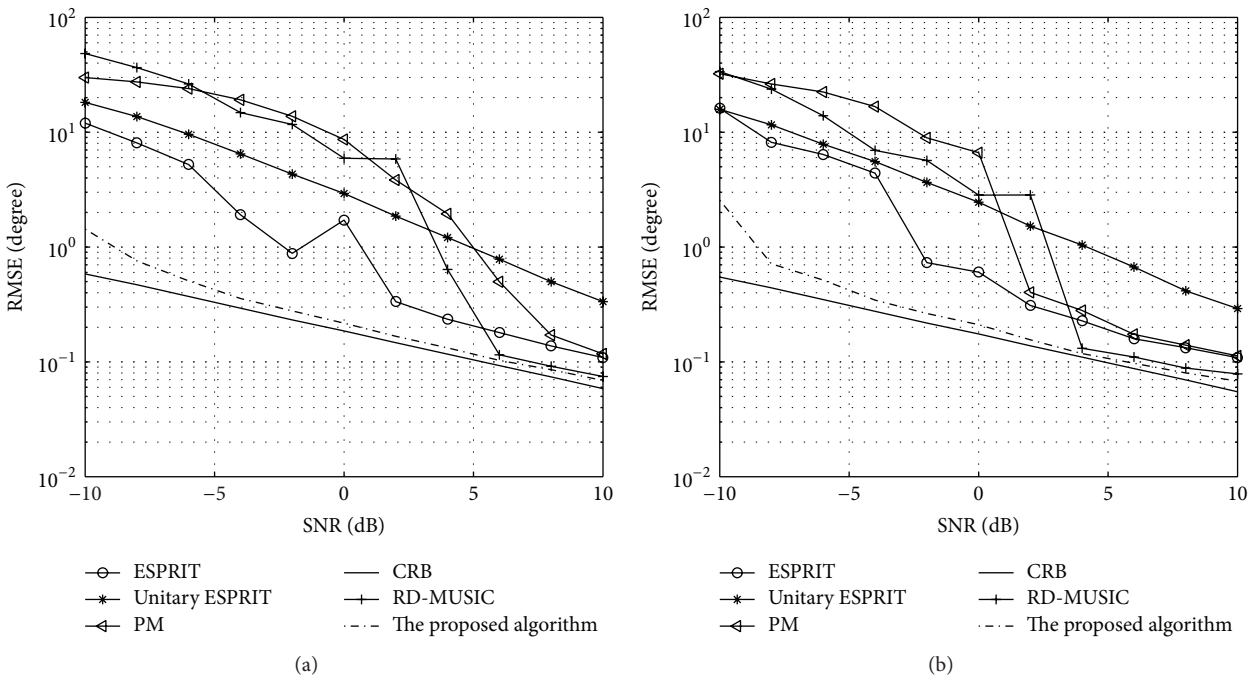

Figure 2: DOD and DOA estimation performance comparison. (a) DOD and (b) DOA.

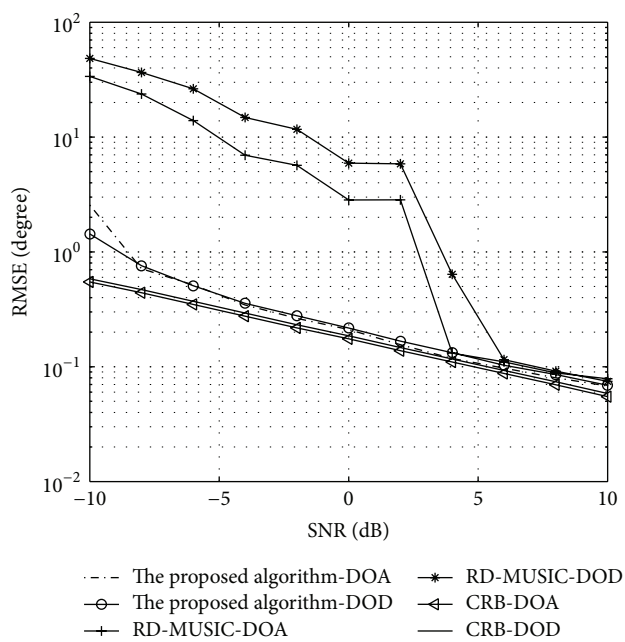

Figure 3: The interference between DOD and DOA estimations.

with the increase of the number of transmit/receive antennas. Multiple transmit/receive antennas improve angle estimation performance because of diversity gain.

Simulation 6 presents the averaged CPU times of the proposed algorithm and RD-MUSIC algorithm with respect to different transmit antennas and receive antennas for DOD and DOA estimation. In this simulation, the number of snapshots is $L = 100$, and the SNR is 0 dB. We consider $P = 3$ uncorrelated targets located at angles $(\theta_1, \varphi_1) = (-15^\circ, -20^\circ)$, $(\theta_2, \varphi_2) = (10^\circ, 45^\circ)$, and $(\theta_3, \varphi_3) = (50^\circ, 5^\circ)$, respectively. As indicated in Table 1, the computational complexity of the proposed algorithm is lower than that of the RD-MUSIC algorithm for identical conditions. This is because the proposed algorithm has a much lower computational complexity owing to estimating the DOD and DOA separately through rearranging the received signal matrix.

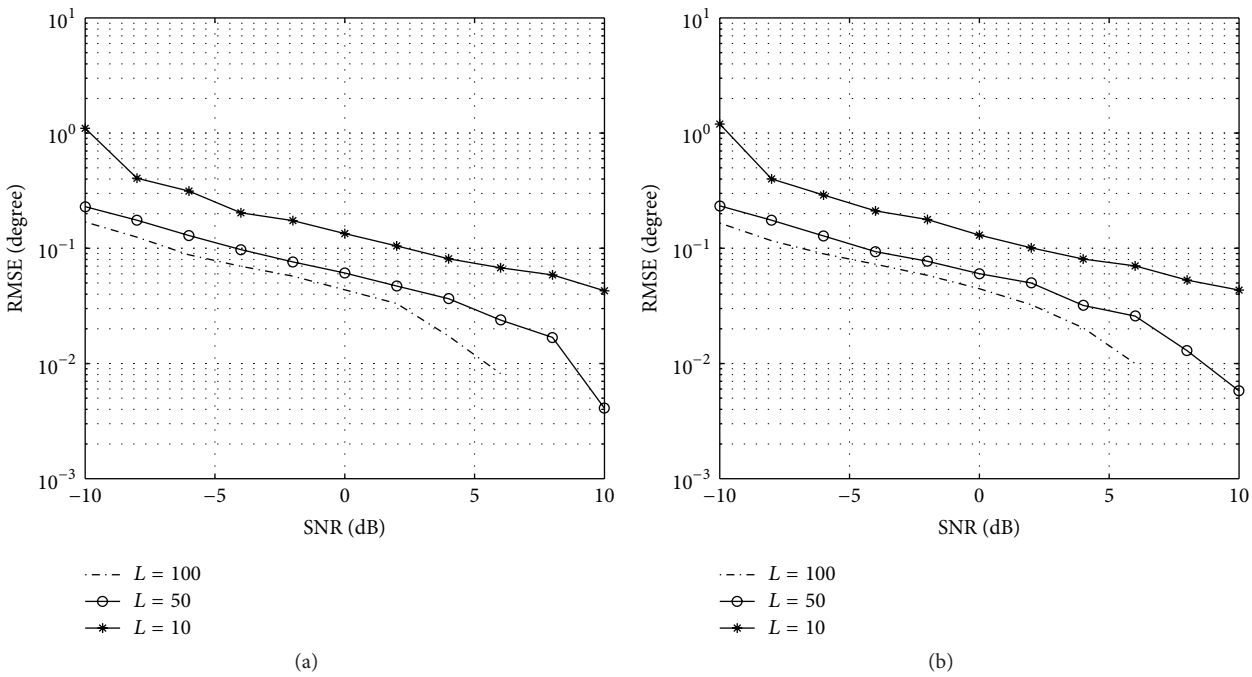

Figure 4: The performance for DOD and DOA estimation with different L. (a) DOD and (b) DOA.

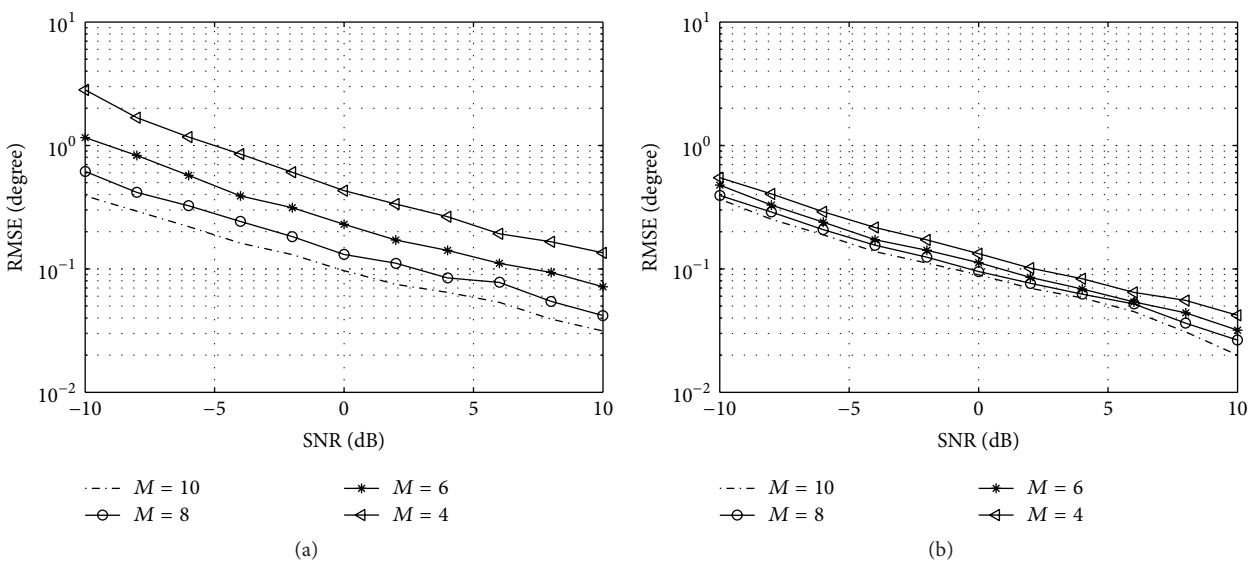

Figure 5: The performance for DOD and DOA estimation with different M. (a) DOD and (b) DOA.

Table 1: Averaged time consumption of the proposed algorithm and RD-MUSIC with respect to M and N. Time unit: sec.

	$M = N =$ 5	$M = N =$ 10	$M = N =$ 15	$M = N =$ 20
The proposed algorithm	0.0413	0.0445	0.0474	0.0559
RD-MUSIC	0.1372	0.3230	0.7925	1.9495

Simulation 7 is used to investigate the performance for multiple coherent targets of the proposed algorithm. In this simulation, we assume a ULA composed of $M = 10$ transmit antennas and $N = 10$ receive antennas. We consider $P = 4$ correlated targets located at angles $(\theta_1, \varphi_1) = (0^\circ, 50^\circ)$, $(\theta_2, \varphi_2) = (45^\circ, 0^\circ)$, $(\theta_3, \varphi_3) = (20^\circ, 30^\circ)$, and $(\theta_3, \varphi_3) = (-25^\circ, -45^\circ)$, respectively. We assume that targets 1 and 2 are fully coherent, and so are targets 3 and 4. In other words, the coherence coefficients matrix is $\begin{bmatrix} 1 & 1 & 0 & 0 \\ 1 & 1 & 0 & 0 \\ 0 & 0 & 1 & 1 \\ 0 & 0 & 1 & 1 \end{bmatrix}$. In this simulation, the number of snapshots is $L = 10$, and the SNR is 0 dB. Figure 7(a) depicts DOD estimation performance of the proposed algorithm for multiple coherent targets. Figure 7(b) presents DOA estimation performance of the proposed algorithm for multiple coherent targets. From the

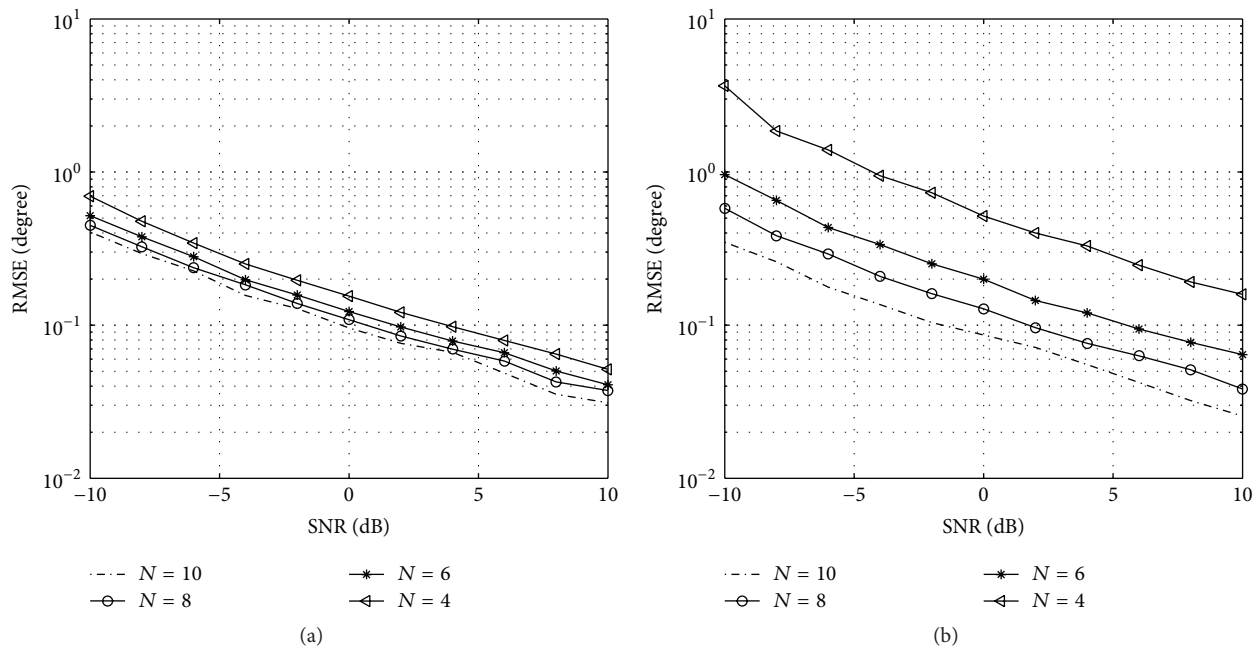

Figure 6: The performance for DOD and DOA estimation with different N. (a) DOD and (b) DOA.

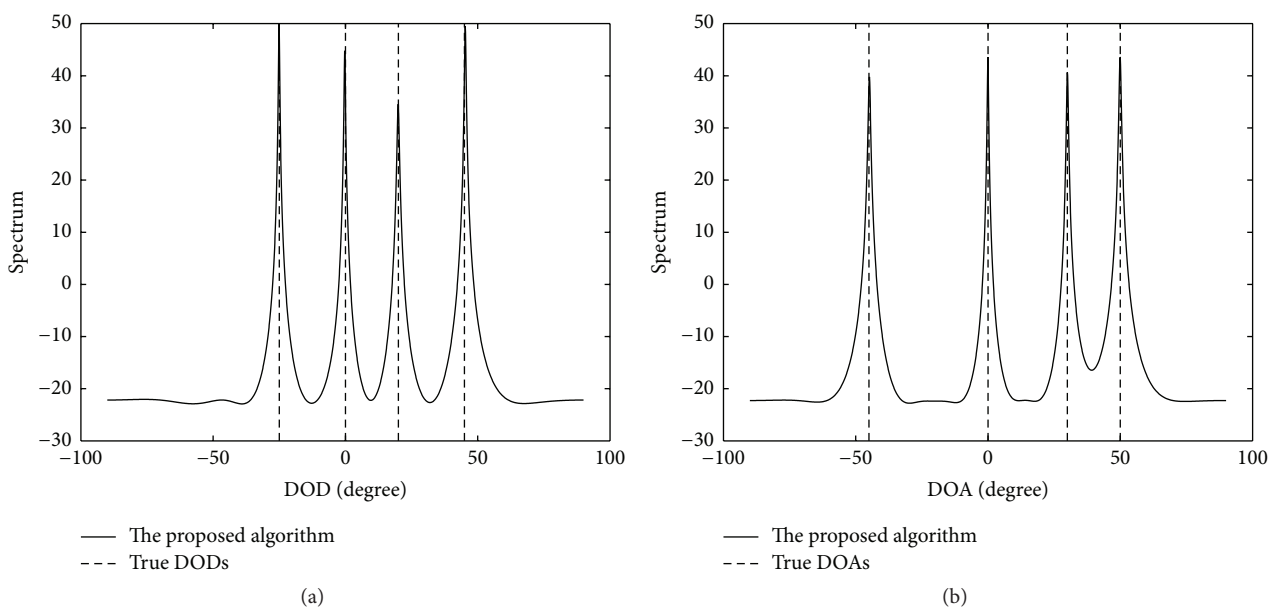

Figure 7: DOD and DOA estimation of multiple coherent targets. (a) DOD and (b) DOA.

figure, we observe that the proposed method can estimate DOD and DOA of coherent targets with good performance.

6. Conclusions

We propose a separate MUSIC algorithm for DOD and DOA estimation in this paper, which guarantees that the DOD and DOA can be estimated separately through rearranging the received signal matrix. Utilizing the separate DOD and DOA estimation, the new algorithm avoids the interference between DOD and DOA estimations in contrast to MUSIC-type algorithms and also achieves lower computational complexity. The main shortcoming of our method is that the working array aperture is reduced, which will result in the loss of degrees of freedom (DOFs). Its number of resolvable targets is only $\min\{M, N\}-1$, rather than well known $MN-1$. Generally, the DOD and DOA estimation performance of the new algorithm will be affected significantly. However, it should be noted that the new algorithm earns more virtual snapshots in return for the DOFs. Hence, the DOD and DOA

estimation performance will be greatly enhanced in the case of limited snapshots being available. Another advantage of the new algorithm is that it is also effective for coherent targets (see Simulation 7).

Appendix

Cramer-Rao Bound

According to [27], the CRB for angle estimation can be derived as follows. For the DOD estimation, we have

$$\mathrm{CRB}(\theta) = \frac{\sigma^2}{2L}\left\{\mathrm{Re}\left[\mathbf{D}_t^H \mathbf{\Pi}_A^{\perp} \mathbf{D}_t\right] \odot \mathbf{R}_s^T\right\}^{-1}, \tag{A.1}$$

while, for the DOA estimation, we have

$$\mathrm{CRB}(\varphi) = \frac{\sigma^2}{2L}\left\{\mathrm{Re}\left[\mathbf{D}_t^H \mathbf{\Pi}_A^{\perp} \mathbf{D}_r\right] \odot \mathbf{R}_s^T\right\}^{-1}, \tag{A.2}$$

where

$$\begin{aligned}
\mathbf{D}_t &= \left[\frac{\partial\left(\mathbf{a}_r(\varphi_1) \otimes \mathbf{a}_t(\theta_1)\right)}{\partial\theta_1}, \ldots, \frac{\partial\left(\mathbf{a}_r(\varphi_P) \otimes \mathbf{a}_t(\theta_P)\right)}{\partial\theta_P}\right], \\
\mathbf{D}_r &= \left[\frac{\partial\left(\mathbf{a}_r(\varphi_1) \otimes \mathbf{a}_t(\theta_1)\right)}{\partial\varphi_1}, \ldots, \frac{\partial\left(\mathbf{a}_r(\varphi_P) \otimes \mathbf{a}_t(\theta_P)\right)}{\partial\varphi_P}\right], \\
\mathbf{\Pi}_A^{\perp} &= \mathbf{I}_{MN} - \mathbf{A}\left(\mathbf{A}^H\mathbf{A}\right)^{-1}\mathbf{A}^H,
\end{aligned} \tag{A.3}$$

and $\odot$ stands for Hadamard product.

Competing Interests

The authors declare no competing interests regarding the publication of this paper.

Acknowledgments

This work is supported in part by the National Natural Science Foundation of China (61571211), in part by the Open Research Fund of National Mobile Communications Research Laboratory, Southeast University (2013D08), and in part by the project funded by China Postdoctoral Science Foundation (2015T80509 and 2014M560403).

References

[1] E. Fishler, A. Haimovich, R. S. Blum, L. J. Cimini Jr., D. Chizhik, and R. A. Valenzuela, "Spatial diversity in radars—models and detection performance," *IEEE Transactions on Signal Processing*, vol. 54, no. 3, pp. 823–838, 2006.

[2] I. Pasya, N. Iwakiri, and T. Kobayashi, "Joint direction-of-departure and direction-of-arrival estimation in a UWB MIMO radar detecting targets with fluctuating radar cross sections," *International Journal of Antennas and Propagation*, vol. 2014, Article ID 847815, 15 pages, 2014.

[3] W.-Q. Wang, "Virtual antenna array analysis for MIMO synthetic aperture radars," *International Journal of Antennas and Propagation*, vol. 2012, Article ID 587276, 10 pages, 2012.

[4] A. M. Haimovich, R. S. Blum, and L. J. Cimini, "MIMO radar with widely separated antennas," *IEEE Signal Processing Magazine*, vol. 25, no. 1, pp. 116–129, 2008.

[5] P. Stoica and A. Nehorai, "Performance study of conditional and unconditional direction-of-arrival estimation," *IEEE Transactions on Acoustics, Speech, and Signal Processing*, vol. 38, no. 10, pp. 1783–1795, 1990.

[6] B. Friedlander and A. J. Weiss, "Direction finding in the presence of mutual coupling," *IEEE Transactions on Antennas and Propagation*, pp. 273–284, 1991.

[7] R. O. Schmidt, "Multiple emitter location and signal parameter estimation," *IEEE Transactions on Antennas and Propagation*, vol. 34, no. 3, pp. 276–280, 1986.

[8] Y. Li, S. Gu, and N. Zheng, "MIMO radar transmit beampattern design for DOA estimation with sidelobe suppression," *International Journal of Antennas and Propagation*, vol. 2016, Article ID 1512843, 10 pages, 2016.

[9] C. Yunhe, "Joint estimation of angle and Doppler frequency for bistatic MIMO radar," *Electronics Letters*, vol. 46, no. 2, pp. 170–172, 2010.

[10] Y. D. Guo, Y. S. Zhang, and N. N. Tong, "Beamspace ESPRIT algorithm for bistatic MIMO radar," *Electronics Letters*, vol. 47, no. 15, pp. 876–878, 2011.

[11] J. Li, X. Zhang, R. Cao, and M. Zhou, "Reduced-dimension MUSIC for angle and array gain-phase error estimation in bistatic MIMO radar," *IEEE Communications Letters*, vol. 17, no. 3, pp. 443–446, 2013.

[12] C. Duofang, C. Baixiao, and Q. Guodong, "Angle estimation using ESPRIT in MIMO radar," *Electronics Letters*, vol. 44, no. 12, pp. 770–771, 2008.

[13] C. Jinli, G. Hong, and S. Weimin, "Angle estimation using ESPRIT without pairing in MIMO radar," *Electronics Letters*, vol. 44, no. 24, pp. 1422–1423, 2008.

[14] G. Zheng, B. Chen, and M. Yang, "Unitary ESPRIT algorithm for bistatic MIMO radar," *Electronics Letters*, vol. 48, no. 3, pp. 179–181, 2012.

[15] Z. D. Zheng and J. Y. Zhang, "Fast method for multi-target localisation in bistatic MIMO radar," *Electronics Letters*, vol. 47, no. 2, pp. 138–139, 2011.

[16] W. Xudong, X. Zhang, J. Li, and J. Bai, "Improved ESPRIT method for joint direction-of-arrival and frequency estimation using multiple-delay output," *International Journal of Antennas and Propagation*, vol. 2012, Article ID 309269, 9 pages, 2012.

[17] M. Jin, G. Liao, and J. Li, "Joint DOD and DOA estimation for bistatic MIMO radar," *Signal Processing*, vol. 89, no. 2, pp. 244–251, 2009.

[18] M. L. Bencheikh and Y. Wang, "Joint DOD-DOA estimation using combined ESPRIT-MUSIC approach in MIMO radar," *Electronics Letters*, vol. 46, no. 15, pp. 1081–1083, 2010.

[19] X. Zhang, L. Xu, L. Xu, and D. Xu, "Direction of departure (DOD) and direction of arrival (DOA) estimation in MIMO radar with reduced-dimension MUSIC," *IEEE Communications Letters*, vol. 14, no. 12, pp. 1161–1163, 2010.

[20] P. Stoica, P. Handel, and A. Nehorai, "Improved sequential music," *IEEE Transactions on Aerospace and Electronic Systems*, vol. 31, no. 4, pp. 1230–1239, 1995.

[21] Q. Cheng and Y. Hua, "Performance analysis of the MUSIC and pencil-MUSIC algorithms for diversely polarized array," *IEEE Transactions on Signal Processing*, vol. 42, no. 11, pp. 3150–3165, 1994.

[22] J. Li, X. Zhang, and W. Chen, "Root-MUSIC based angle estimation for MIMO radar with unknown mutual coupling," *International Journal of Antennas and Propagation*, vol. 2014, Article ID 918964, 8 pages, 2014.

[23] Y. Zhang and Z. Ye, "Efficient method of DOA estimation for uncorrected and coherent signals," *IEEE Antennas and Wireless Propagation Letters*, vol. 7, pp. 799–802, 2008.

[24] F. Belfiori, W. Van Rossum, and P. Hoogeboom, "Coherent MIMO array design with periodical physical element structures," *IEEE Antennas and Wireless Propagation Letters*, vol. 10, pp. 1341–1344, 2011.

[25] Y.-H. Choi, "Subspace-based coherent source localisation with forward/backward covariance matrices," *IEE Proceedings—Radar, Sonar and Navigation*, vol. 149, no. 3, pp. 145–151, 2002.

[26] S. U. Pillai and B. H. Kwon, "Forward/backward spatial smoothing techniques for coherent signal identification," *IEEE Transactions on Acoustics, Speech, and Signal Processing*, vol. 37, no. 1, pp. 8–15, 1989.

[27] P. Stoica and A. Nehorai, "MUSIC, maximum likelihood, and Cramer-Rao bound," *IEEE Transactions on Acoustics, Speech, and Signal Processing*, vol. 37, no. 5, pp. 720–741, 1989.